

## Determination of Doping Density in GaAs Semiconductor by Wavelength-Dependent Photoacoustic Spectroscopy<sup>†</sup>

Jong-Tae Lim,<sup>b</sup> Ok-Lim Choi, Doo Wan Boo,<sup>a,\*</sup> and Joong-Gill Choi<sup>a,\*</sup>

Department of Chemistry, Yonsei University, Seoul 120-749, Korea

\*E-mail: dwboo@yonsei.ac.kr (D. W. Boo); jgchoi@yonsei.ac.kr (J.-G. Choi)

Received October 2, 2013, Accepted October 7, 2013

The wavelength dependence of the photoacoustic signal for n-type GaAs semiconductors in the region of the band-gap energies was investigated. The significant changes in the phase and amplitude of the photoacoustic signal near the band-gap absorption wavelengths were observed to occur when the Si-doping densities in GaAs were varied. Particularly, the first derivatives of the photoacoustic phase vs. wavelength graphs were evaluated and fitted with single Gaussian functions. The peak centers and the widths of the Gaussian curves clearly showed linear relationships with the log values of the Si-doping densities in n-type GaAs semiconductors. It is proposed that the wavelength-dependent PA spectroscopy can be used as a simple and nondestructive method for measuring the doping densities in bulk semiconductors.

**Key Words :** Photoacoustics, Wavelength-dependent phase, GaAs, Doping density, Nondestructive detection

### Introduction

The optical interactions with matters resulting in the generation of the heat come under the general heading of photothermal phenomena, and the experimental methods utilizing such interactions are known as photoacoustic (PA) and photothermal techniques. The PA signal depends on the optical absorption coefficient of the material, the light-into-heat conversion efficiency, and the thermal transport properties. Thus the PA spectroscopic technique has been widely utilized to investigate the non-radiative de-excitation and photo-induced thermal conversion processes. The PA spectroscopic techniques have also proven to be a very sensitive tool for studying the thermal properties of materials<sup>1-5</sup> such as thermal diffusivity and thermal conductivity with sufficient accuracy.<sup>6-8</sup> In addition, various PA techniques have been applied to measure the composition-dependent optical energy gap, optical absorption coefficient, and thermal properties and carrier transport properties in glasses,<sup>9-11</sup> alloys,<sup>12</sup> metal oxides,<sup>13</sup> ion implantations,<sup>14,15</sup> and semiconductors.<sup>16-22</sup> However almost no measurement was yet accomplished for the determination of the doping density in semiconductor materials by the use of the PA method.

The conventional methods for measuring the doping densities in semiconductor materials include the photoluminescence method<sup>23,24</sup> and the capacitance method.<sup>25,26</sup> These techniques have been successfully employed to investigate the band-gap shifts and band-gap tailing behaviors of vari-

ous doped semiconductors. Due to their limited applications and complicated experimental conditions, however, it is desirable to develop a simple but more general photo-absorption technique for measuring doping densities that can be also applied to optically opaque materials.

Recently, we have succeeded in applying the PA method to the doped semiconductors, and revealed the linear dependence of the PA signal on the doping density of bulk semiconductors in the modulation frequency region where the non-radiative bulk recombination is dominant.<sup>27</sup> In this paper, we propose another PA method for determining Si-doping densities in bulk GaAs by analyzing wavelength-dependent PA phases and amplitudes near the band-gap energies.

### Experimental

The specific characteristics of bulk GaAs samples used in our experiment are shown in Table 1. All the Si-doped GaAs samples were ~350 μm thick for precise comparison and the doping densities were varied from ~10<sup>16</sup> cm<sup>-3</sup> to ~10<sup>18</sup> cm<sup>-3</sup>. The front and back of the samples had mirror-like and etched rough surfaces, respectively. Figure 1 shows a schematic diagram of the experimental setup used in this study. A Ti:sapphire laser (Coherent Inc. Model 890) pumped by Ar<sup>+</sup>

**Table 1.** Sample characteristics of intrinsic GaAs and n-type GaAs with three Si-doping densities

Sample	Si-Doping Density (cm <sup>-3</sup> )	Thickness (μm)	Surface finish (Front/Back)
Int. GaAs	-	350	Polished/Etched
A	1.0 × 10 <sup>16</sup>	350	Polished/Etched
B	2.7 × 10 <sup>17</sup>	351	Polished/Etched
C	1.4 × 10 <sup>18</sup>	350	Polished/Etched

<sup>†</sup>This paper is to commemorate Professor Myung Soo Kim's honourable retirement.

<sup>a</sup>These authors contributed equally to this work.

<sup>b</sup>Present address: Samsung Advanced Institute of Technology, Samsung Electronics Co. LTD. 97, Samsung 2-Ro, Gyeonggi-Gu, Yong-In Si, Gyeonggi-Do 446-712, Korea

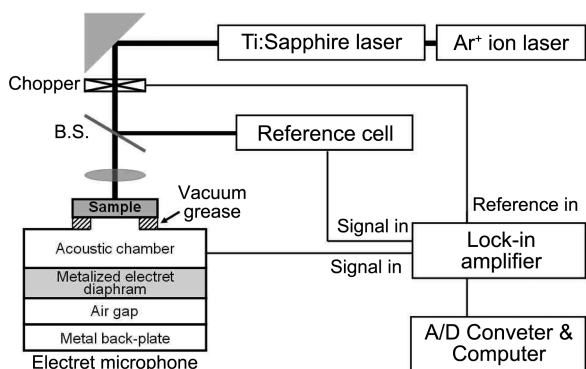


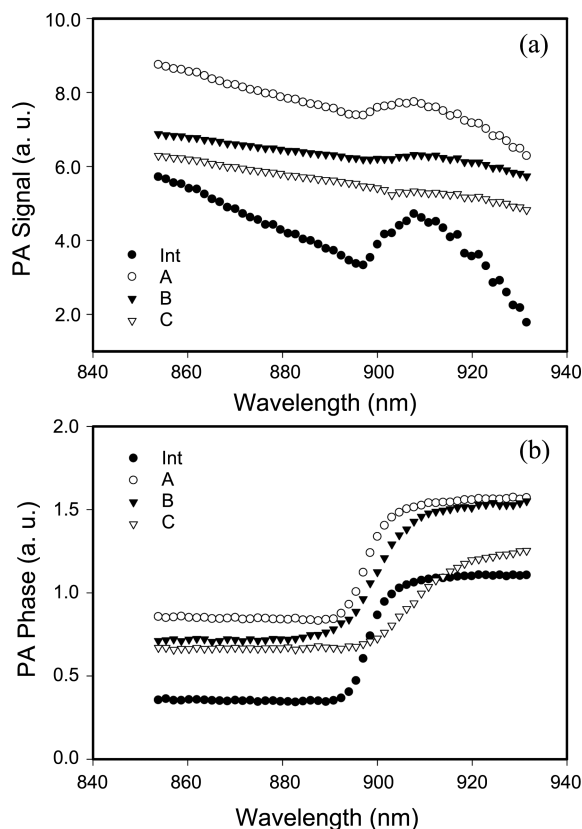
**Figure 1.** Schematic diagram of the experimental setup for wavelength-dependent photoacoustic measurements

laser (Coherent Inc. Model INNOVA 305) was operated in the spectral ranges of 850–930 nm. The laser power was adjusted to 20 mW by using a neutral density filter to maintain the experimental condition for linear optical absorption of the GaAs semiconductors. Since the thermal diffusivity of the GaAs material was  $\sim 0.46 \text{ cm}^2/\text{sec}$ , the incident beam was modulated by a mechanical chopper (EG&G PARC Model 197) at 2 kHz in order to satisfy a thermally thick condition.<sup>4,28</sup>

A minimal volume cell, similar to open PA cell proposed by Miranda *et al.*,<sup>29</sup> was employed to measure the PA signals. The front-sound inlet had a circular hole of 2 mm in diameter and the front-sound air chamber, adjacent to the metallized face of the diaphragm, was  $\sim 1$  mm in length. The samples were mounted directly onto the front sound inlet of an electret microphone (Radio Shack Inc. Model 270-092B). The PA signal from the microphone was detected by a lock-in amplifier (EG&G PARC Model 5210) coupled with a preamplifier (EG & G PARC 122) and further processed with a personal computer.

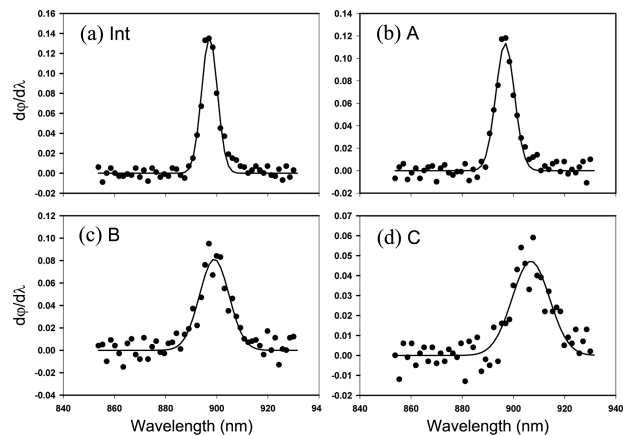
## Results and Discussion

Figure 2 shows the wavelength-dependent amplitude and phase of PA signal for the intrinsic GaAs and doped GaAs samples with three different Si densities, normalized with a carbon black as a reference. In the figure, there are three features to be noted. First, the significant changes in the amplitude and phase of the PA signal are observed to occur near the band-gap energies ( $\sim 900$  nm). Second, the observed band-gap energy of intrinsic GaAs is red-shifted from the literature value (1.43 eV at 300 K) corresponding to 870 nm in wavelength.<sup>29</sup> It is believed that the red-shift is caused by the heating effects by near-IR absorption used in this experiment. It is well-known that the band-gap energy of the semiconductors tends to decrease as the temperature increases. Third, as the Si-doping densities in GaAs are varied, the spectral shapes and magnitudes of the PA phases change more systematically than those of the PA amplitudes. This suggests that the spectral characteristics of the PA phase near the band-gap energy could have strong correlation with the Si-doping densities in GaAs.



**Figure 2.** PA spectra of various n-type GaAs samples with different Si-doping densities: (a) PA amplitude and (b) PA phase.

To investigate the dependence of the PA phase on the doping density, the first derivatives of the phase shift ( $\phi$ ) with respect to the wavelength  $\lambda$  (*i.e.*  $d\phi/d\lambda$ ) are evaluated and fitted with single Gaussian functions, as shown in Figure 3. The resulting Gaussian curves for four GaAs samples are compared in Figure 4. They clearly show that both the peak centers and the widths of the Gaussian curves change systematically according to the Si-doping densities in GaAs. Table 2 summarizes the peak centers and the full width half



**Figure 3.** Differential values of the PA phase vs. wavelength along with Gaussian curve fitting in (a) intrinsic GaAs, (b) sample A, (c) sample B, and (d) sample C.

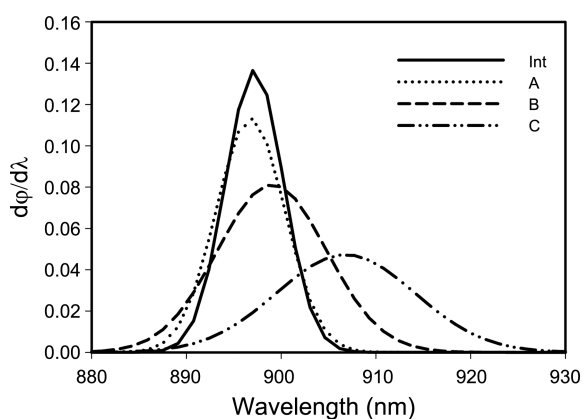


**Figure 4.** Comparison of curve fittings in PA phase for various Si doping densities in GaAs semiconductors.

**Table 2.** Values of the peak center and FWHM from Gaussian curve fitting of PA phase for n-type GaAs semiconductors

	Int. GaAs	A	B	C
Center (nm)	897.2	896.8	899.1	906.8
FWHM (nm)	7.2	8.5	13.6	17.2

maxima (FWHM) in the Gaussian curves of the PA phase for various Si-doping densities in n-type GaAs. It is noteworthy that as the Si-doping density in GaAs is increased, the peak center and the FWHM of the Gaussian curve are more red-shifted and more widened, respectively, from those of intrinsic GaAs sample. The observed trends are attributed to the band-gap energy narrowing and band tailing behaviors of impurity-doped semiconductors. It has been previously reported that the band-gap narrowing and band tailing behaviors are mostly originated from electron-electron exchange interactions and electron-phonon interactions involving structurally disordered impurities, respectively and are also well-known for Si-doped n-type GaAs semiconductors. For instance, the observed red-shifts of the peak centers in Table 2 are somewhat similar to the predicted band-gap narrowing ( $\sim 6$  nm) at the Si-doping densities used in the experiment.

Figure 5 shows the empirical relationship between the Si-doping density and the spectroscopic values of Table 2. In the figure, the peak centers and the FWHM of the Gaussian curves are plotted with respect to the log values of Si-doping densities. It is clearly demonstrated that the spectral characteristics of the Gaussian curves possess a linear relationship with the log values of the Si-doping densities. In particular, the FWHM of the Gaussian curves (Fig. 5(b)) corresponding to the slope of the PA phase vs. wavelength graph (in Fig. 2(b)) near the band-gap shows strong correlation with the Si-doping densities. This suggests that the measurement of the wavelength-dependent PA phase near the band-gap energies can be used for determining the doping density in semiconductors with reasonable accuracy.

Finally, the origin for the strong correlation observed between the changes in the PA phase near the band-gap and the Si-doping densities in GaAs can be explained qualitatively

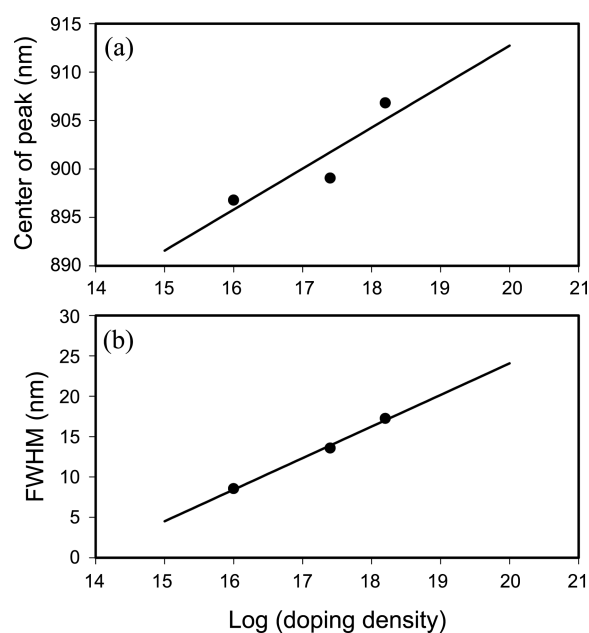


**Figure 5.** Plots of (a) peak center and (b) FWHM of the fitted Gaussian curves for PA phase with respect to the log values of Si-doping densities.

as follows. It is known that as the doping density in n-type semiconductors increases, the electron-electron and electron-impurity ion interactions increases resulting in more enhanced band-gap narrowing and band-tailing (known as Urbach tailing). Due to the presence of more scattering centers and the increased structural disorder, the non-radiative recombination rate for the photoexcited carriers also increases. As a result, in the photoabsorption process of direct band-gap semiconductors like GaAs, the absorption coefficients at energies below the band-gap are non-zero, and generally described by exponentially decaying functions with the doping-dependent slopes. On the other hand, according to the thermal diffusion model<sup>2-5</sup> of the PA process for thermally thick sample used in this experiment, the PA phase depends strongly on the non-radiative recombination lifetime that tends to decrease with increasing doping density. Importantly, the shapes of PA phase spectra near and below the band-gap, when the absorption coefficients are not too high, are expected to follow those of the photoabsorption spectra. This suggests that the shapes of the PA phase spectra near the band-gap wavelengths contain the spectral signatures of the dopant-induced band-gap narrowing and band-tailing. It is noteworthy that there also exists similar correlation between the FWHM of the photoluminescence peak and the doping density in n-type InP semiconductor.<sup>30</sup>

## Conclusion

In this paper, it is demonstrated that the wavelength-dependent photoacoustic spectroscopy near the band-gap energies can be used as a simple and non-destructive method in determining the doping densities in n-type GaAs semiconductors. The observed changes in the photoacoustic phase

and amplitude near the band-gap energies are analyzed by evaluating the first derivatives that can be correlated with the Si-doping densities in GaAs. The peak centers and the widths of the fitted Gaussian curves clearly show the linear relationships with the log values of the Si-doping densities in GaAs. Particularly, the FWHM of the Gaussian curves corresponding to the slope of the PA phase vs. wavelength graph near the band-gap are found to have better correlation with the Si-doping densities in n-type GaAs semiconductors.

**Acknowledgments.** This research was supported by Basic Science Research Program through the National Research Foundation of Korea (NRF) funded by the Ministry of Education, Science and Technology (NRF-2009-0072984 and NRF-2012-8-0661).

### References

- Smith, W. L.; Rosencwaig, A.; Willenborg, D. L.; Opsal, J.; Taylor, M. W. *Solid State Technology* **1986**, 29, 85.
- Vargas, H.; Miranda, L. C. M. In *Photoacoustic and Thermal Wave Phenomena in Semiconductors*; Mendelis, A., Ed., North-Holland: New York, 1987; p 141.
- Vargas, H.; Miranda, L. C. M. *Phys. Rep.* **1988**, 161, 43.
- Rosencwaig, A. *Photoacoustics and Photoacoustic Spectroscopy*; Wiley: New York, 1980.
- Mandelis, A., Ed., *Progress in Photothermal and Photoacoustic Science and Technology*; Elsevier: New York, 1992; Vol. 1.
- Marinelli, M.; Zammit, U.; Schudieri, F.; Martellucci, S. *Il Nuovo Cimento* **1987**, 9D, 855.
- Pao, Y. *Optoacoustic Spectroscopy and Detection*; Academic Press: New York, 1977.
- Ferreira, S. O.; Ying An, C.; Bandeira, I. N.; Miranda, L. C. M. *Phys. Rev. B* **1989**, 39, 7967.
- Shen, Q.; Kato, Y.; Toyoda, T. *Jpn. J. Appl. Phys.* **1997**, 36, 3297.
- Ghosh, A. K.; Chaudhuri, B. K. *J. Appl. Phys.* **1996**, 80(9), 5292.
- Ghosh, A. K.; Chaudhuri, B. K. *J. Appl. Phys.* **1996**, 79(2), 723.
- Pichardo, J. L.; Marin, E.; Alvarado-Gil, J. J.; Mendoza-Alvarez, J. G.; Cruz-Orea, A.; Delgadillo, I.; Torres-Delgado, G.; Vagas, H. *Appl. Phys. A* **1997**, 65, 69.
- Toyoda, T.; Shiozaki, I. *Materials Science and Engineering : B* **1996**, 41, 102.
- Kuwahata, H.; Uehara, F.; Matsumori, T.; Muto, N. *Nucl. Instr. and Meth. in Phys. Res. B* **1997**, 127/128, 459.
- Zegadi, A.; Al-Saffar, I. S.; Yakushev, M. V.; Tomlinson, R. D. *Rev. Sci. Instrum.* **1995**, 66(8), 4095.
- Toyoda, T.; Shinoyama, K. *Jpn. J. Appl. Phys.* **1997**, 36, 3300.
- Ferreira da Silva, A.; Veissid, N.; An, C. Y.; Pope, I.; Barros de Oliveira, N.; Batista da Silva, A. V. *Appl. Phys. Lett.* **1996**, 69(13), 1930.
- Felici, A. C.; Lama, F.; Piacentini, M.; Papa, T.; Debowska, D.; Kisiel, A.; Rodzik, A. *J. Appl. Phys.* **1996**, 80(12), 6925.
- Bandeira, I. N.; Closs, H.; Ghizoni, C. C. *J. Photoacoustics* **1982**, 1, 275.
- (a) Neto, A. P.; Vargas, H.; Leite, N. F.; Miranda, L. C. M. *Phys. Rev. B* **1990**, 41, 9971. (b) Miranda, L. C. M. *Appl. Opt.* **1982**, 21, 2923.
- Mikoshiba, N.; Nakamura, H.; Tsubouchi, K. in *Proceedings of the IEEE Ultrasonics Symposium*, San Diego, IEEE, New York, 1982; p 580.
- Sablikov, V. A.; Sandomirskii, V. B. *Phys. Status Solidi* **1983**, 120, 471.
- Borghs, G.; Ghattacharyya, K.; Deneffe, K.; Van Mieghem, P.; Mertens, R. *J. Appl. Phys.* **1989**, 66(9), 4381.
- Lowney, J. R. *J. Appl. Phys.* **1986**, 60(8), 2854.
- Van Mieghem, P.; Mertens, R. P.; Borghs, G.; Van Overstraeten, R. *J. Phys. Rev. B* **1990**, 41, 5952.
- Bennett, H. S. *J. Appl. Phys.* **1986**, 60(8), 2866.
- Lim, J. T.; Choi, J. G.; Noh, S. K.; Je, K. C.; Yim, S. Y.; Park, S. H. *Jap. J. Appl. Phys.* **2007**, 46, 7888.
- Sze, S. M. *Physics of Semiconductor Devices*, 2nd ed.; John Wiley & Sons: New York, 1981; p 851.
- Perondi, L. F.; Miranda, L. C. M. *J. Appl. Phys.* **1987**, 62, 2955.
- Bugajski, M.; Lewandowski, W. *J. Appl. Phys.* **1985**, 57, 521.